



# Synergistic therapy of magnetism-responsive hydrogel for soft tissue injuries

Lining Zhang<sup>a,1</sup>, Xiuqin Zuo<sup>a,1</sup>, Shengjie Li<sup>a,1</sup>, Mi Sun<sup>b</sup>, Huimin Xie<sup>a</sup>, Kai Zhang<sup>a</sup>, Jikun Zhou<sup>a</sup>, Liyun Che<sup>a</sup>, Junxuan Ma<sup>d,e</sup>, Zishan Jia<sup>a,\*\*</sup>, Fei Yang<sup>b,c,\*</sup>

<sup>a</sup> Rehabilitation Medicine Department, PLA General Hospital, Beijing, 100853, China

<sup>b</sup> Beijing National Laboratory for Molecular Sciences, State Key Laboratory of Polymer Physics & Chemistry, Institute of Chemistry, Chinese Academy of Sciences, Beijing, 100190, China

<sup>c</sup> School of Chemistry and Chemical Engineering, University of Chinese Academy of Sciences, Beijing, 100049, China

<sup>d</sup> Orthopedic Research Institute, The First Affiliated Hospital of Sun Yat-sen University, Guangzhou, China

<sup>e</sup> Guangdong Provincial Key Laboratory of Orthopedics and Traumatology, Guangzhou, China

## ARTICLE INFO

### Keywords:

Hydrogel

Magnetism-responsive

Tissue injury

Tetra-PEG/agar

## ABSTRACT

Soft tissue injury is very common and associated with pain, tissue swelling and even malformation if not treated on time. Treating methods include cryotherapy, electrical therapy, ultrasound therapy and anti-inflammatory drug, but none of them is completely satisfying. In this work, for a better therapeutic effect, drug therapy and pulsed electromagnetic field (PEMF) therapy were combined. We constructed a drug delivery system using the tetra-PEG/agar hydrogel (PA). By incorporating Fe<sub>3</sub>O<sub>4</sub> NPs into the hydrogel network, a magnetism-responsive property was achieved in the system. The cytotoxicity and *in vivo* study showed a good biocompatibility of the PA/Fe<sub>3</sub>O<sub>4</sub> hydrogel. A magnetism-controlled release was attained by the incorporation of Fe<sub>3</sub>O<sub>4</sub>. Finally, *in vivo* study showed a better performance of the DS-loaded PA/Fe<sub>3</sub>O<sub>4</sub> compared with the commercially available DS ointment regarding the recovery of the injured soft tissue. Therefore, this magnetism-responsive hydrogel may represent a promising alternative to treat soft tissue injury.

## 1. Introduction

Soft tissue injury is a common problem usually leading to pain, swelling and sometimes even malformation [1,2]. On-time treatment is vital to improve clinical outcome. Current treatments include cryotherapy, electrical therapy, ultrasound therapy and anti-inflammatory drug therapy and can promote healing [3,4]. However, the treatment for soft tissue injury is still a big challenge in clinical practise as the curative effects of the above methods are not satisfactory [2,5]. Synergistic therapy is a widely explored method to improved curative effects for cancer therapy [6,7], which possesses improved curative effects compared with the cures using single drug or way. However, this method has been rarely explored in the treatment of injured soft tissues.

Diclofenac sodium (DS) is a nonsteroidal anti-inflammatory drug, and is used to treat soft tissue injury due to its effectiveness and safety [1,8,9]. Studies have demonstrated that DS could penetrate the skin and distribute to the target tissue underlying the application site [8,10,11]. Generally, the commercially available DS is DS ointment, which cannot

control the release of the drugs, resulting in dose-dependent problems, such as gastrointestinal, dermatological and the central nervous system toxicity [12,13]. As a result, a more efficient, safer drug delivery system is needed. Hydrogel have long been adopted as drug delivery system, among which the *in situ* hydrogel possess the advantage of simple drug formulation and the ability to deliver both hydrophilic and hydrophobic drugs [14]. However, due to irregular shapes, like legs and arms, the *in situ* hydrogel is of problem that can flow down before the gelation.

Pulsed electromagnetic field therapy has already been a clinical method to accelerate tissue healing and recovery [15]. Researches have suggested that PEMF could reduce pain via its effect on nitric oxide (NO), calmodulin (CaM), and/or opioid pathways, and it's also a potential method to treat soft tissue injury [15].

In this work, we prepared a hydrogel dressing combining DS with PEMF therapy to treat soft tissue injury (Scheme 1). Firstly we applied the tetra-PEG hydrogel that have been widely used as the drug delivery system because they could be easily formed by the dual-syringes

Peer review under responsibility of KeAi Communications Co., Ltd.

\* Corresponding author. Institute of Chemistry, Chinese Academy of Sciences, Zhongguancun North First Street 2, Beijing, 100190, China.

\*\* Corresponding author.

E-mail addresses: [JZS1963@163.com](mailto:JZS1963@163.com) (Z. Jia), [fyang@iccas.ac.cn](mailto:fyang@iccas.ac.cn) (F. Yang).

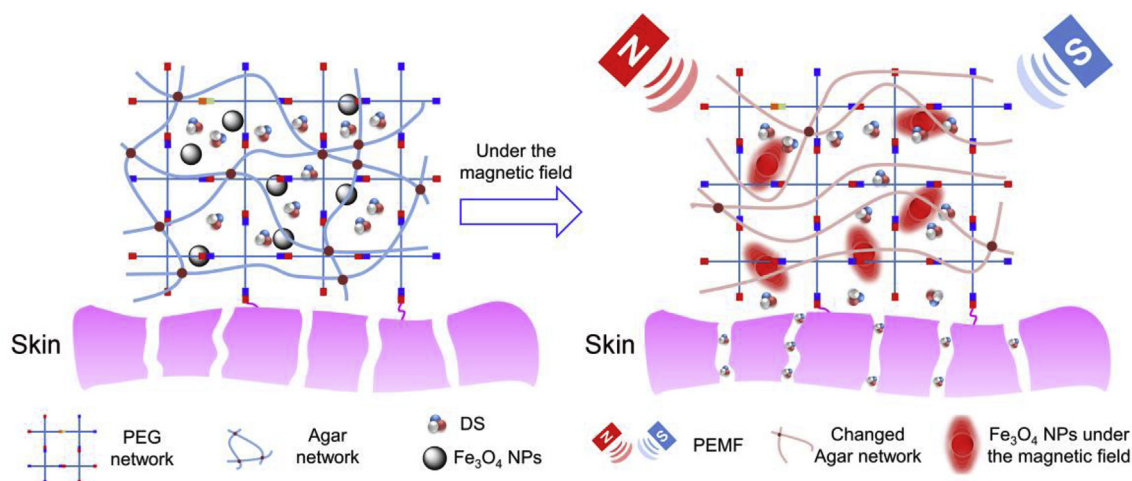
<sup>1</sup> These authors equally contributed to this work.

<https://doi.org/10.1016/j.bioactmat.2019.03.002>

Received 15 January 2019; Received in revised form 24 March 2019; Accepted 25 March 2019

Available online 12 April 2019

2452-199X/ This is an open access article under the CC BY-NC-ND license (<http://creativecommons.org/licenses/by-nc-nd/4.0/>).



**Scheme 1.** Schematic for formation of tetra-PEG/agar hydrogel/Fe<sub>3</sub>O<sub>4</sub>/DS (PA/Fe<sub>3</sub>O<sub>4</sub>/DS) system for the synergetic therapy of soft tissue injury.

injection [16]. Although the crosslinking rate between PEG-NH<sub>2</sub> and PEG-NHS is fast, the precursor solutions still easily flow down the tissue before gelation. To avoid flowing and make the precursor solution more viscous, agar, a safe, cheap and commonly used agent to increase the viscosity in 3D printing, was incorporated into the network [17,18]. Moreover, we also added Fe<sub>3</sub>O<sub>4</sub> NPs into the network to get the responsive release of DS in PEMF [19]. Under the tuned magnetic field, Fe<sub>3</sub>O<sub>4</sub> NPs would on one hand shake back and forth to accelerate the drug release and on the other hand generate heat to change the agar network and speed up the release [20,21]. In addition, *in vitro* cell experiments and *in vivo* implanting experiments were carried out to test the biocompatibility of the dressing. The magnetism-responsive release of the hydrogel was also examined by *in vitro* and *in vivo* experiments. The synergistic therapeutic effect was evaluated by animal experiments. All the results proved that the dressing might be a promising candidate in the treatment of soft tissue injury.

## 2. Experimental section

### 2.1. Materials

4-Armed poly(ethylene glycol) succinimidyl (Tetra-PEG-NHS,  $M_w = 20$  kDa,  $M_w/M_n = 1.03$ ) and 4-armed poly(ethylene glycol) amine (Tetra-PEG-NH<sub>2</sub>,  $M_w = 20$  kDa,  $M_w/M_n = 1.03$ ) were purchased from SINOPEG, China. Agar was purchased from ENERGY CHEMICAL. Ferric acetylacetonate (Fe(acac)<sub>3</sub>), 1,2-hexadecanediol, oleylamine, oleic acid, and polyol medium triethylene glycol were purchased from J & K Scientific Ltd. All chemicals were used as received. All other chemicals were of analytical grade.

### 2.2. Synthesis and characterization of water-soluble Fe<sub>3</sub>O<sub>4</sub> NPs

The water-soluble Fe<sub>3</sub>O<sub>4</sub> NPs were prepared according to previous literature [22]. Briefly, Fe(acac)<sub>3</sub> (1 mmol, 99%, Acros) and polyol medium triethylene glycol (30 mL) were mixed together and slowly heated to reflux (278 °C) for 30 min under argon protection, producing a black homogeneous colloidal suspension. After cooled down to room temperature, 20 mL of ethyl acetate was added to the reaction solution, resulting in a black precipitation of magnetite nanoparticles which was then separated from the solution by a magnetic field. After being washed by ethyl acetate for three times, the precipitation was re-dispersed in water for further use.

### 2.3. Preparation of the hydrogel

The hydrogel was prepared in the phosphate buffer solution (pH

7.4) as previous reported [23]. Briefly, agar (200 mg, melting point 80 °C) was added into a tube with 10 mL of PBS and heated to 80 °C in an oil bath. After being heated for several minutes, the transparent agarose solution was cooled down to 40 °C, and then diclofenac sodium (100 mg/mL) and (5.44 wt%) Fe<sub>3</sub>O<sub>4</sub> NPs were added to the mixture. Next, precursor solution 1 was prepared by dissolving Tetra-PEG-NH<sub>2</sub> (8 wt%) with the mixed solution in a sample bottle, and precursor solution 2 (8 wt%) was prepared by dissolving Tetra-PEG-NHS in another sample bottle with the mixed solution. By using dual syringe, the same volume of precursor solution 1 and 2 were simultaneously injected into the molds and then cooled down at room temperature to form hydrogel. The syringe was heated to 40 °C in the oven before use.

### 2.4. Scanning electron microscopy

The hydrogels were prepared as described above and then freeze-dried at -50 °C for 48 h. Then the samples were carefully stuck onto the conducting resin with double-sided adhesive, and sputter-coated with a thin layer of Pt for 90 s to make the sample conductive before testing. Field emission scanning electron microscopy (SEM) images were obtained at acceleration voltage of 5 kV on a JSM-6700F microscope (JEOL, Japan).

### 2.5. Torsion experiments

The hydrogels were used as dressings and their adhesion to porcine skin was evaluated according to previous report [24]. The porcine skin was used because it's biologically similar to human skin. First, the hydrogels were formed in situ on the surface of the skin by using a dual syringe, and then torsion stress was applied on the hydrogels to test their adherence flexibility on the skin.

### 2.6. In vitro drug release study

Only one side of the hydrogel would touch the skin during drug release process, so we employed the same release model as reported previously [14]. The hydrogel was prepared in a container with the diameter of 10 mm and height of 2 mm, and diclofenac sodium was encapsulated inside the hydrogel. Then, the drug-contained hydrogel was immersed into the PBS (7.4) and the solutions were collected at special intervals of time. During each interval, the magnetic field was applied for 30 min. The collected solution at different time were tested using the UV-visible spectroscopy (276 nm). The release without the PEMF was set as control.

## 2.7. *In vivo* drug release study

The drug-containing hydrogel was formed *in situ* on the surface of the rats' skin (SD rats). During each interval, the rats were treated with or without the PEMF for 30 min. Then the hydrogel-located tissues were collected at 2, 6 and 12 h. Next, the collected tissues were treated with tissue destructor, and methyl alcohol was used to extract the diclofenac sodium. After adding methyl alcohol into the tissue, supernatant was collected after centrifuge, and was then passed through a 0.45  $\mu\text{m}$  pore-sized filter. The filtered supernatant was evaluated using the high performance liquid chromatography (HPLC, C18 Reversed-phase chromatography, detection wavelength 276 nm, mobile phase methanol: water: acetic acid = 90:10:0.25).

## 2.8. *In vitro* cytotoxicity

The cytotoxicity of the hydrogel was studied by the CCK-8 assay. Firstly, extraction of the hydrogel was obtained by immersing the hydrogel (1 g) into the Dulbecco's modified Eagle medium (DMEM) (1 mL). The 3T3 mouse fibroblasts were plated in 96-well cell culture plate at a density of  $10^4$  cells/well, incubated with the extraction under 5%  $\text{CO}_2$  at 37 °C for 1 and 3 days and then changed to 100  $\mu\text{L}$  of fresh DMEM. Subsequently, 10  $\mu\text{L}$  of CCK-8 was added to each well to incubate at 37 °C for 4 h in a  $\text{CO}_2$  incubator. Finally, 100  $\mu\text{L}$  of the solutions was put into a new 96-well plate. The optical density of each well at 570 nm (reference 650 nm) was read by a microplate reader.

## 2.9. *In vivo* biocompatibility

The *in vivo* biocompatibility was evaluated by implanting the hydrogel into rat tissue subcutaneously. The hydrogel disks (5 mm in diameter and 1 mm in height) were put subcutaneously on the back of the rats. At specific times, the rats were sacrificed. The hydrogels along with surrounding tissue were collected and soaked in formalin for 3 days. After that, the samples were embedded in paraffin, cut into 3–5  $\mu\text{m}$  slices and stained with H&E. The histological imaging was performed using an Olympus microscopy.

## 2.10. Animal model of soft tissue injury

SD rats of 150 g were used in this study. The soft tissue injury was created in the back of the rats by dropping a weight (50 g) from the height of 15 cm for 10 times. Then, the injured rats were treated by the hydrogel dressing with and without the PEMF (0.3 T) and DS ointment. Finally, after special times, the rats were euthanized, and the injured tissues were collected for H&E staining.

## 3. Results and discussion

### 3.1. Characterization of water-soluble $\text{Fe}_3\text{O}_4$ NPs

To combine magnet therapy with drug therapy, we introduced the magnetic  $\text{Fe}_3\text{O}_4$  NPs into the hydrogel network. The  $\text{Fe}_3\text{O}_4$  NPs must be water-soluble to incorporate into the hydrogel network after dispersing in the precursor water solutions of the hydrogel. The water-soluble NPs were prepared according to previous report by a simple and cheap method based on a polyol process [22]. Fig. 1A and B showed that the NPs were nearly monodispersed with the diameter of 10 nm. Due to the intrinsic magnetic properties, the NPs would aggregate at the high-field site [25]. Fig. 1C showed that when a magnet was placed next to the  $\text{Fe}_3\text{O}_4$  NPs, the NPs aggregated near the magnet, clearly demonstrating the intrinsic magnetic property of the  $\text{Fe}_3\text{O}_4$  NPs.

### 3.2. Preparation of drug-loaded magnetism-responsive PA hydrogel

Since the surface of the wound is generally irregular, the *in situ*

hydrogels such as tetra-PEG hydrogel, have the advantage to cover the whole wound. During the experiment, we found that tetra-PEG hydrogel gelled a little slowly (longer than 20 s) that can flow down before gelled. To solve the problem, we incorporated biocompatible agar into the hydrogel network to increase the viscosity of the precursor solution before the complete gelation. The obtained hydrogel was of porous structure (Fig. 2A) that will benefit nutrient exchange and drug release [26].  $\text{Fe}_3\text{O}_4$  NPs and diclofenac sodium could be incorporated into the hydrogel easily *in situ* by mixing with the precursor solution. The SEM of the obtained hydrogel with  $\text{Fe}_3\text{O}_4$  NPs and diclofenac sodium was shown in Fig. 2B. After loading the drugs and the  $\text{Fe}_3\text{O}_4$  NPs, we could observe some aggregates that may be explained by aggregation of the  $\text{Fe}_3\text{O}_4$  NPs and the DS. But the hydrogel remained porous, indicating their morphology did not changed. When leveraged as dressings, the hydrogel must be able to adhere to the skin without any outside pressure. We used tetra-PEG-NHS to construct the hydrogel, which could react with the  $\text{NH}_2$  from tissue protein [27]. Fig. 2C showed that, despite the torsion, the hydrogel could still adhere to the porcine skin tightly, proving the good adherence and the potential to be used as plasters.

### 3.3. Cell viability and biocompatibility

The constructing materials of the hydrogel were PEG hydrogel and the agar. PEG hydrogel was used extensively in scaffolds for engineering applications like articular cartilage, neural tissue, and bladder tissue regeneration [28–31]. Agar has already been adopted as the matrix for cell culture [32,33]. Besides, both PEG and agar have been approved by FDA, so the resulting dressings should be nontoxic. To prove that, cell viability experiments were carried out through the NIH 3T3 mouse fibroblast cells and showed over 90% of cell viability even after three days of culture (Fig. 3A). Besides, we tested the cytotoxicity of hydrogel with  $\text{Fe}_3\text{O}_4$  NPs and DS, and still showed the materials were nontoxic.

To demonstrate biocompatibility *in vivo*, subcutaneous implanting experiments was performed. At certain time, the rats were euthanized and tissue samples were harvested for histological analysis (Fig. 3B). A slight inflammatory response could be observed after 7 days of implantation (Fig. 3C), which might result from foreign body reaction. However, 14 days later, the inflammatory cell density decreased with large amounts of fibroblasts appeared, indicating the resolving inflammatory response. The increased fibroblasts would produce the collagen needed for the wound healing [34]. 28 days later, the inflammatory cells could not be observed indicating the inflammation resolved. *In vivo* study also showed a good biocompatibility for the hydrogel.

### 3.4. *In vitro* drug release

For synergistic effect of treatment, drugs were incorporated, of which the release can be controlled by extra magnetic field. Under PEMF, the shaking of the  $\text{Fe}_3\text{O}_4$  NPs in the network would add force to the network to increase the release speed, and the effect would be enhanced when the hydrogel was porous. In addition, heat can be generated to further accelerate the drug release [25]. To prove that, we carried out the *in vitro* release experiments. Considering that only one side of the hydrogel would contact the injured soft tissue, the PA/ $\text{Fe}_3\text{O}_4$ /DS was put in the receptacle with the diameter of 15 mm and height of 3 mm so that only one side was accessible to the release medium (Fig. 4A). The UV absorption of the release medium at different time was recorded to test the released DS. Fig. 4B showed that the release speed under the magnet field was higher. The total release amount under the magnetic field was  $72.3 \pm 2.6\%$  compared to only  $51.6 \pm 3.0\%$  without magnetic field. The release experiments demonstrated that drug release could be tuned by the magnetic field, which provided the possibility to combine the physical and drug

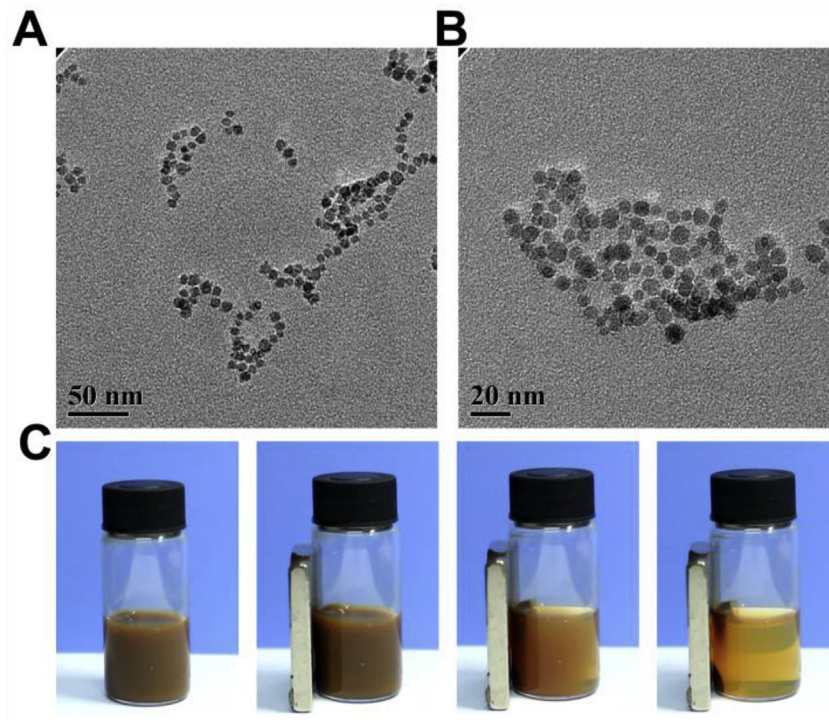


Fig. 1. Characterization of the water-soluble  $\text{Fe}_3\text{O}_4$  NPs. (A, B) TEM images of  $\text{Fe}_3\text{O}_4$  NPs. (C) Pictures showing that  $\text{Fe}_3\text{O}_4$  NPs could be attracted by the magnet.

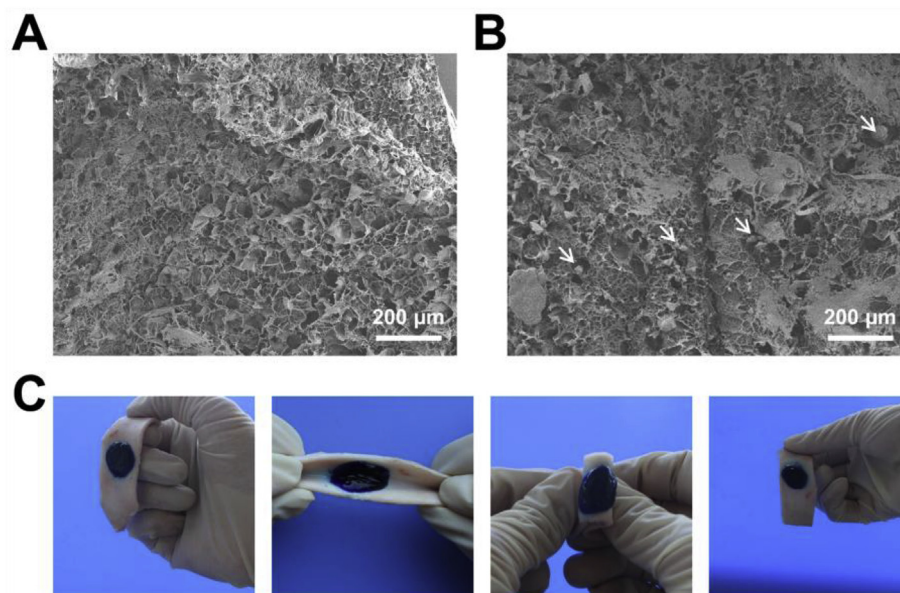


Fig. 2. The SEM images of the PA hydrogel (A) and the PA/ $\text{Fe}_3\text{O}_4$ /DS hydrogel (B). The arrows indicated the aggregated DS and  $\text{Fe}_3\text{O}_4$  NPs. (C) Pictures of torsion experiments showed that the PA/ $\text{Fe}_3\text{O}_4$ /DS hydrogel could adhere to the tissue tightly. The methyl blue was incorporated for better viewing.

therapy.

### 3.5. *In vivo* release experiments

*In vivo* release experiment was performed to confirm the *in vitro* results. Firstly, the dressings gelled *in situ* on the back of the rats (Fig. 5A and B), and the influence of extra magnetic field on the release was evaluated. In this experiment, the commercially available DS ointment (Voltaren) was used as control. The amount of the DS was calculated so that all the groups contained the same amount of loaded DS. After experiments, the tissues next to the dressings were collected, grinded and then extracted with methyl alcohol. Fig. 5C showed that

the release amount of the DS ointment-treated skins was the largest ( $22.8 \pm 2.4 \mu\text{g/mL}$ ) at the initial 2 h while those of the PA/ $\text{Fe}_3\text{O}_4$ /PEMF and PA/ $\text{Fe}_3\text{O}_4$  were  $19.6 \pm 2.2$  and  $12.7 \pm 2.7 \mu\text{g/mL}$  respectively. It could be deduced that in a drug delivery system, the PA dressing could decrease the bursting release of the drugs observed in an ointment system. Six hours later, PA/ $\text{Fe}_3\text{O}_4$ /PEMF-treated skin had the largest amount of drug, which was maintained even after 12 h. As the control, the drug concentration of the DS ointment-treated groups kept decreasing from  $20.1 \pm 2.1$  to  $15.7 \pm 2.2 \mu\text{g/mL}$ . Although the PA/ $\text{Fe}_3\text{O}_4$ -treated groups had the lowest drug concentration, it could still offer a stable drug concentration during the testing. The *in vivo* release experiments showed that compared with the commercially available DS

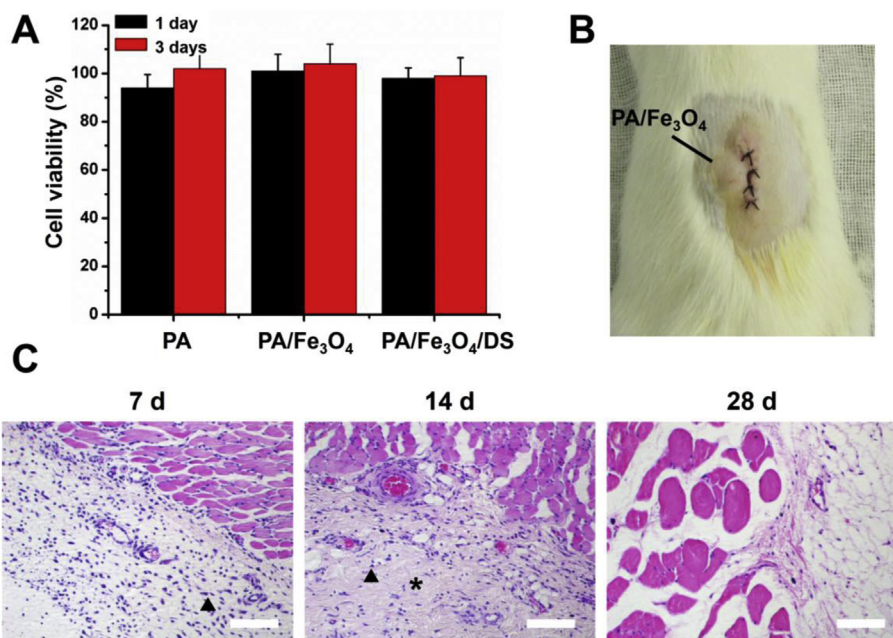


Fig. 3. (A) The relative cell viability of PA, PA/Fe<sub>3</sub>O<sub>4</sub> and PA/Fe<sub>3</sub>O<sub>4</sub>/DS. (B) The picture of the subcutaneous implanting experiments. (C) H&E staining results of the subcutaneous implanting experiments after 7, 14 and 28 days. The triangles indicated the inflammatory cells and the asterisks indicated the fibroblasts. Bar scales = 200 μm.

ointment, the PA/Fe<sub>3</sub>O<sub>4</sub> dressings could achieve a steadier drug release. Besides, when adding magnetic field, the drug concentration could be improved. In our experiments, it was surprising to find one out of six rats treated by DS ointment died at the first 2 h, and presumably it was triggered by the complications of the diclofenac sodium that might lead to side effects in gastrointestinal, dermatological and the central nervous system, because the concentration was too high [12,13].

### 3.6. Animal model of soft tissue injury

To further test the efficacy of the PA/Fe<sub>3</sub>O<sub>4</sub> hydrogel for soft tissue repair, the soft tissue injury model of the rats was established by hitting a weight (50 g) from 15 cm high for ten times (Fig. 6A) on the back of the rat. To confirm the injured tissue, the broken skin was collected for histological analysis. As shown in Fig. 6B, before the skin was hit by the weight, the muscle tissue was dense and continuous; after hit they were mal-aligned because of the damage. Besides, blood cells could be observed because the injury of vessels and is the early sign of the inflammation response after being wounded [35]. The broken muscle, blood cells infiltration and the inflammation clearly declared the successful modelling of the injured soft tissue.

Using the above models, the PA/Fe<sub>3</sub>O<sub>4</sub>/DS gelled in situ on the surface of the wound, and the rats were treated with or without the magnetic field. Also, the rats treated with the commercially available DS ointment were used as a control (Fig. 7A). Again, in this experiment, some animals died after using the DS ointment. Fig. 7B revealed that after one day of treatment, the PA/Fe<sub>3</sub>O<sub>4</sub>/DS-treated groups had relatively larger unhealed part, while the DS ointment showed better result than the PA/Fe<sub>3</sub>O<sub>4</sub>/DS with more healed part of the muscles. However, the PA/Fe<sub>3</sub>O<sub>4</sub>/DS/PEMF achieved the smallest area of defect in all the groups. Three days later, it was nearly impossible to see the defect in the PA/Fe<sub>3</sub>O<sub>4</sub>/DS/PEMF groups and seven days later, the muscle tissue became continuous almost the same as the healthy tissue in Fig. 6B. There were still some defects in the PA/Fe<sub>3</sub>O<sub>4</sub>/DS and DS ointment treated groups at day 3 and the smoothness and continuity were not comparable with PA/Fe<sub>3</sub>O<sub>4</sub>/DS/PEMF-treated group. The animal experiment illustrated that after the combination of magnet therapy with drug therapy, PA/Fe<sub>3</sub>O<sub>4</sub>/DS dressing accelerated healing of injured soft tissue, which was superior to commercially available DS ointment.

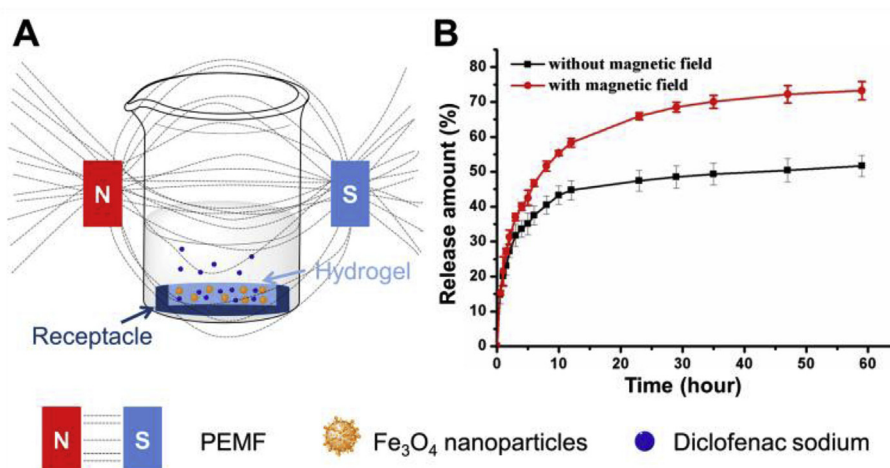
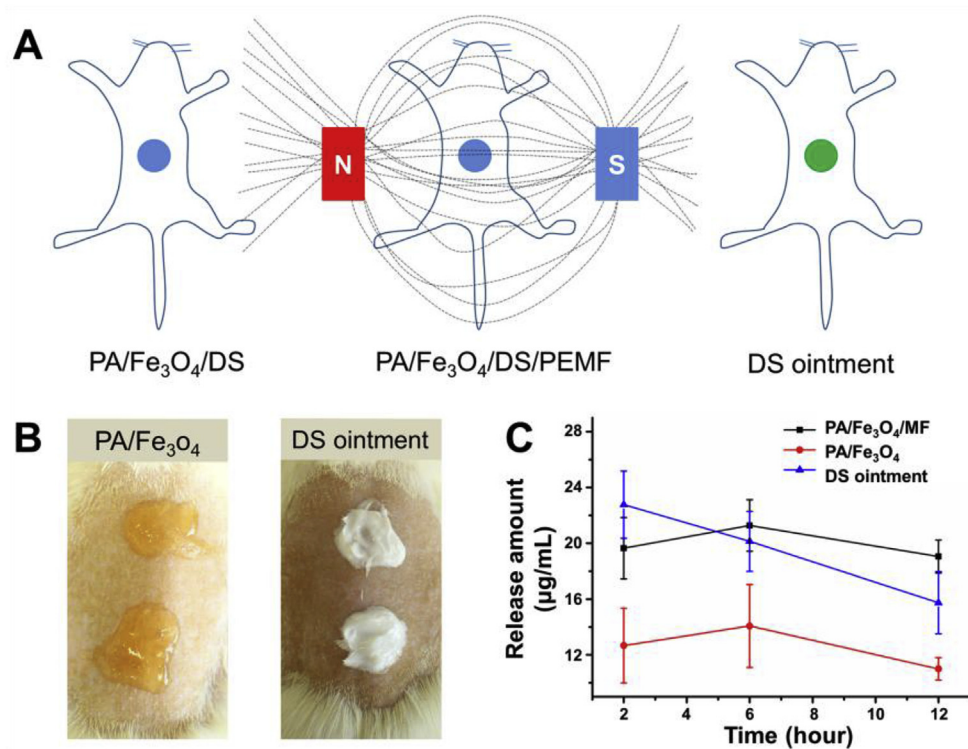


Fig. 4. (A) Schematic showing the *in vitro* release experiments. (B) The release profiles of the dressing with (red) or without (black) the PEMF.



**Fig. 5.** (A) Schematic showing the *in vivo* release experiments. The PA/Fe<sub>3</sub>O<sub>4</sub> dressing formed in situ on the back of the rats and release happened without (PA/Fe<sub>3</sub>O<sub>4</sub>/DS) or with (PA/Fe<sub>3</sub>O<sub>4</sub>/DS/PEMF) the magnetic field. The commercially available DS ointment was used as a control. (B) Pictures showing the PA/Fe<sub>3</sub>O<sub>4</sub> dressings and the DS ointment on the back of the rats. (C) Results of the *in vivo* release experiments.

#### 4. Conclusions

In summary, we prepared a new hydrogel dressing from Tetra-PEG hydrogel, agar and Fe<sub>3</sub>O<sub>4</sub> NPs for the synergistic therapy of magnetic and drug. The *in vitro* and *in vivo* evaluation showed a good biocompatibility. The release experiments proved the magnetism-responsive release function. Finally, the animal experiments showed that the dressing under the magnet field promoted a better tissue repair than the commercialized DS ointment. The hydrogel seems to be a promising

candidate to improve treatment of the injured tissue.

#### Notes

The authors declare no competing financial interests.

#### Acknowledgment

We gratefully acknowledge NSFC (51573195), Program of

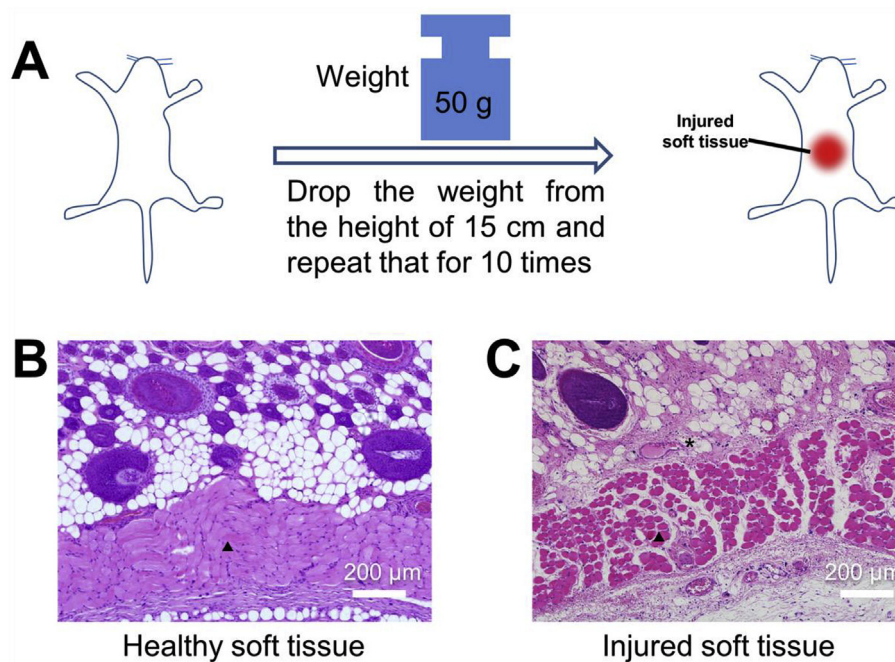


**Fig. 6.** (A) The schematic diagram showed the modelling process of the injured soft tissue on the back of rats. (B, C) H&E staining of the healthy and injured muscles. The triangles indicated the muscle tissue and the asterisks indicated the expanded vessels.

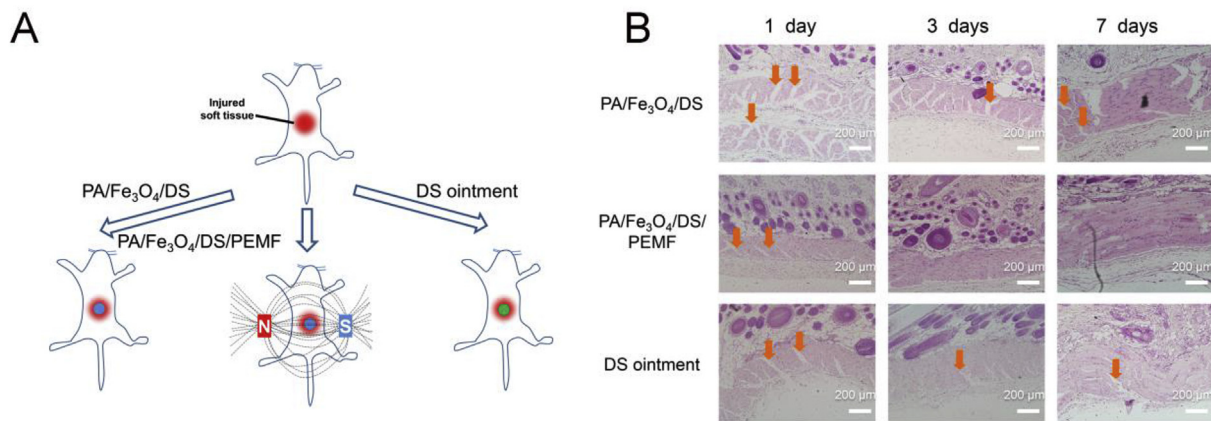


**Fig. 7.** (A) Schematic showed the animal experiments. (B) The H&E staining results of the injured soft tissue after being treated with the PA/Fe<sub>3</sub>O<sub>4</sub>/DS, PA/Fe<sub>3</sub>O<sub>4</sub>/DS/PEMF and the commercialized DS ointment after 1, 3 and 7 days. The yellow arrows indicate the defects of the muscle.

transformation medicine of PLA General Hospital (2016TM-039) for financial support.

## References

- [1] P. de Almeida, S.S. Tomazoni, L. Frigo, P.D.C. de Carvalho, A.A. Vanin, L.A. Santos, G.M. Albuquerque-Pontes, T. Marchi, O. Tairova, R.L. Marcos, R.A.B. Lopes-Martins, E.C.P. Leal, *Laser Med. Sci.* 29 (2014) 653–658.
- [2] S. Ball, M. Halaki, R. Orr, *Br. J. Sports Med.* 51 (2017) 1012–U52.
- [3] H.-G. Predel, B. Giannetti, M.P. Connolly, F. Lewis, A. Bhatt, *Postgrad. Med.* 130 (2018) 24–31.
- [4] K.A. Stanford, L. Phillips, Y.C. Chang, D. Leemon, T. Schimelpfenig, N.S. Harris, *Wilderness Environ. Med.* 28 (2017) 307–312.
- [5] G.L. Lanzi, *Clin. Sport. Med.* 36 (2017) 287–298.
- [6] X.F. Ding, X. Xu, Y. Zhao, L.H. Zhang, Y.D. Yu, F. Huang, D.Z. Yin, H. Huang, *RSC Adv.* 7 (2017) 35086–35095.
- [7] Y.Y. Xiao, Y.P. Yang, Y.J. Wu, C.M. Wang, H. Cheng, W. Zhao, Y. Li, B.B. Liu, J.L. Long, W.H. Guo, G.P. Gao, M.L. Gou, *RSC Adv.* 7 (2017) 32613–32623.
- [8] H.G. Predel, H. Pabst, A. Schaefer, D. Voss, N. Giordan, *J. Sports Med. Phys. Fitness* 56 (2016) 92–99.
- [9] P. de Almeida, R.A.B. Lopes-Martins, S.S. Tomazoni, G.M. Albuquerque-Pontes, L.A. Santos, A.A. Vanin, L. Frigo, R.P. Vieira, R. Albertini, P. d. C. de Carvalho, E.C.P. Leal, *Photochem. Photobiol.* 89 (2013) 501–507.
- [10] J.M.M. Vidart, T.L. da Silva, P.C.P. Rosa, M.G.A. Vieira, M.G.C.J. da Silva, *Appl. Polym. Sci.* 135 (2018) 45919.
- [11] T.C. Lima, E. Bagordakis, S.G. Moreira Faldi, C.R. Rocha dos Santos, M.L. Pimenta Pinheiro, *J. Oral Surg.* 76 (2018) 60–66.
- [12] M. Giovannetti, M.A. Machado, M. Borrelli Junior, C.I. Ikejiri, N. Alonso, P.D. Branco, *Rev. Hosp. Clin.* 48 (1993) 39–42.
- [13] D.F. Zandstra, C.P. Stoutenbeek, J.P. Alexander, *Intensive Care Med.* 9 (1983) 21–23.
- [14] Y.Z. Bu, L.C. Zhang, J.H. Liu, L.H. Zhang, T.T. Li, H. Shen, X. Wang, F. Yang, P.F. Tang, D.C. Wu, *ACS Appl. Mater. Interfaces* 8 (2016) 12674–12683.
- [15] R. Waniphakdeedecha, A. Sathaworawong, W. Manuskiatti, N.S. Sadick, *J. Cosmet. Laser Ther.* (2017) 1–5.
- [16] T. Sakai, T. Matsunaga, Y. Yamamoto, C. Ito, R. Yoshida, S. Suzuki, N. Sasaki, M. Shibayama, U. i. Chung, *Macromolecules* 41 (2008) 5379–5384.
- [17] X.C. Yang, Z.H. Lu, H.Y. Wu, W. Li, L. Zheng, J.M. Zhao, *Mater. Sci. Eng. C, Mater. Biol. Appl.* 83 (2018) 195–201.
- [18] K.D. Roehm, S.V. Madhally, *Biofabrication* 10 (2018) 015002.
- [19] A.H. Rezayan, M. Mousavi, S. Kheirjou, G. Amoabediny, M.S. Ardestani, J. Mohammadnejad, *J. Magn. Magn. Mater.* 420 (2016) 210–217.
- [20] O.S. Manoukian, M.R. Arul, N. Sardashti, T. Stedman, R. James, S. Rudraiah, S.G.J. Kumbar, *Appl. Polym. Sci.* 135 (2018) 46068.
- [21] C. Zhang, H.C. Luan, G.Y. Wang, *J. Appl. Polym. Sci.* 135 (2018) 46112.
- [22] J. Wan, W. Cai, X. Meng, E. Liu, *Chem. Commun.* (2007) 5004–5006.
- [23] Y.Z. Bu, H. Shen, F. Yang, Y. Yang, X. Wang, D.C. Wu, *ACS Appl. Mater. Interfaces* 9 (2017) 2205–2212.
- [24] C. Ghobril, K. Charoen, E.K. Rodriguez, A. Nazarian, M.W. Grinstaff, *Angew. Chem. Int. Ed.* 52 (2013) 14070–14074.
- [25] S.J. Xu, F. Yang, X. Zhou, Y.P. Zhuang, B.X. Liu, Y. Mu, X. Wang, H. Shen, G. Zhi, D.C. Wu, *ACS Appl. Mater. Interfaces* 7 (2015) 20460–20468.
- [26] Z.J. Fan, B. Liu, J.Q. Wang, S.Y. Zhang, Q.Q. Lin, P.W. Gong, L.M. Ma, S.R. Yang, *Adv. Funct. Mater.* 24 (2014) 3933–3943.
- [27] I. Strehin, Z. Nahas, K. Arora, T. Nguyen, J. Elisseeff, *Biomaterials* 31 (2010) 2788–2797.
- [28] M. Mehdizadeh, H. Weng, D. Gyawali, L.P. Tang, J. Yang, *Biomaterials* 33 (2012) 7972–7983.
- [29] R.R. Yang, C.X. Xu, T. Wang, Y.Q. Wang, J.N. Wang, D.P. Quan, D.Y.B. Deng, *RSC Adv.* 7 (2017) 41098–41104.
- [30] E.T. Tenorio-Neto, D. d. S. Lima, M.R. Guilherme, M.K. Lima-Tenorio, D.B. Scariot, C.V. Nakamura, M.H. Kunita, A.F. Rubira, *RSC Adv.* 7 (2017) 27637–27644.
- [31] H. Seo, S.G. Heo, H. Lee, H. Yoon, *RSC Adv.* 7 (2017) 28684–28688.
- [32] H. Yin, X. Shi, H. Wang, W. Jin, Y. Li, Y. Fu, *RSC Adv.* 7 (2017) 50562–50570.
- [33] Z.P. Wu, R.F. Guan, M. Tao, F. Lyu, G.Z. Cao, M.Q. Liu, J.G. Gao, *RSC Adv.* 7 (2017) 12437–12445.
- [34] Y. Liu, H. Meng, S. Konst, R. Sarmiento, R. Rajachar, B.P. Lee, *ACS Appl. Mater. Interfaces* 6 (2014) 16982–16992.
- [35] M. Shahriarsalamat, *J. Neuropathol. Exp. Neurol.* 69 (2010).